Output feedback control for a nonlinear optical interferometry system

Gerardo Flores, *Member, IEEE*, and Micky Rakotondrabe, *Member, IEEE*

***Abstract*— In an interferometer system, the interferometer's phase stores essential information of an object of interest. Hence, one of the fundamental optical interferometry problems is to estimate such a phase (aka signal of interest). Another critical issue in the interferometry is the interferometer's stabilization. In this work, we propose a nonlinear observer that estimates the interferometer phase signal. Besides, we design a nonlinear control algorithm that globally stabilizes the interferometer to any of the stable equilibrium points. For that aim, we only use the output voltage, a piece of the usually available information in any interferometer. This fact results in an output feedback control scheme. A rigorous stability analysis is presented together with simulations that corroborate the theoretical results.**

***Index Terms*— Interferometer, Lyapunov stability, nonlinear observer, optics, output feedback control.**

I. Introduction

Optical interferometry is now accessible to a wide range of engineers, optical researchers, manufacturers, and even astronomers. Especially for astronomers, interferometry provides a powerful new tool to unlock the secrets of the universe [1]. For example, a black hole was photographed for the 1st time in 2019 [2]. As one can imagine, optical interferometry is science relevant for nowadays applications. One of the most crucial interferometry problems aims to answer the following question. How do we estimate the phase of a signal given by an interferometer? Several methods have been proposed to answer this question; most of them are the so-called phase-shifting algorithms [3]. On the other hand, another problem is stabilizing interferometers. Usually, in the interferometry literature control system approach is rarely used for such stabilization and only relies on simple linear control methods [4], [5], [6], [7]. This paper proposes a method based on control theory to robustly stabilize an interferometer while accurately estimate the phase of the signal with a nonlinear state estimator algorithm. For that aim, we first develop a dynamic model that represents the interferometer. Then, we propose a control strategy to stabilize the interferometer.

Manuscript received August 31, 2020; revised November 10, 2020; accepted November 29, 2020. Date of publication **XXXX**; date of current version December 13, 2020. Recommended by Senior Editor Giovanni Cherubini. *(Corresponding author: Gerardo Flores.)*

G. Flores is with the Laboratorio de Percepción y Robótica (LAPyR), Center for Research in Optics, Loma del Bosque 115, León, Guanajuato, 37150 Mexico (e-mail: gflores@cio.mx).

Micky Rakotondrabe is with the Laboratoire Génie de Production, National School of Engineering in Tarbes (ENIT - INPT), University of Toulouse, Tarbes, France. (e-mail: mrakoton@enit.fr).

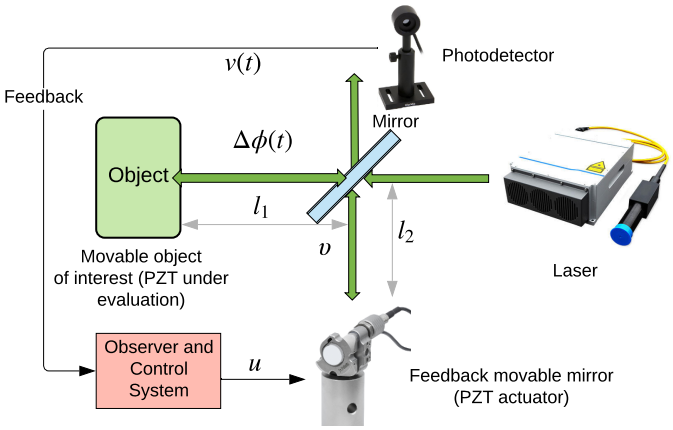

Fig. 1. Block diagram of the Michelson interferometer with a control system in the loop. There are two mobile devices: the PZT piezoelectric actuator and a movable object of interest.

A. Related work

Several works implemented different techniques to obtain the phase from a given interferometer. For instance, in [8], the authors experimentally performed adaptive phase estimation using time-symmetric quantum smoothing for a varying phase on a continuous wave coherent beam. In [9], the authors presented an interferometric phase control capable of locking any chosen phase value. However, this approach is heuristic, and the results are not mathematically demonstrated. The latter is the case of the vast majority of works that deal with interferometric phase estimation and control. One of the most relevant results is [10], where authors improved a telescope's interferometric imaging performance. The authors used classical control theory to estimate a telescope's mirror motions. In particular, they used a Luenberger observer.

Further, the authors of [11] described a phase-shifting interferometric algorithm using an arbitrary phase step. The algorithm characterized a piezo-actuator[1] nonlinearity and precisely estimated the vibration-induced during piezoelectric transducer translation. Assuming no error in the PZT, six data frames were sufficient to estimate the correct phase steps. Contrary to [11], we will estimate the phase without using data frames; indeed, we only need a feedback signal from the movable object of interest usually available in experimental benchmarks. Finally, in [12], the authors presented a control system to stabilize an interferometer; however, such a work lacks several mathematical formalisms and does not recover

[1]Lead zirconate titanate piezoelectric transducer, shortened PZT.

the interest signal. In our work, we solve those problems.

B. Contribution

In the vast majority of the interferometry works, estimation and observer theory is not implemented nor considered. Moreover, nonlinear control algorithms are rarely applied; besides, these rare works usually do not provide mathematical proof that formally supports their results [12], [10]. In term of interferometry modeling, two main approaches are popular from the optics community: the phase-shifting algorithms operating in the time domain [13], and that of the frequency domain [14]. Also, it is prevalent that in such papers, the authors use an algebraic interferometer mathematical model. Using that model and classic optic techniques, the signal of interest, i.e., the interferometer phase, is obtained. This interferometer phase contains the required information to characterize the object of interest [15].

We start studying the well-known interferometer algebraic model. From that model, we build the interferometer dynamics. In particular, the studied model can represent the *Michelson Interferometer* [15], [16]. In the Michelson interferometer, we consider two mobile devices: the PZT actuator permitting a feedback laser beam; and a movable object of interest which can be represented by another PZT actuator, see Fig. 1. Once we have modeled the Michelson Interferometer dynamics, we propose a robust nonlinear control algorithm based on variable structure systems [17], [18] to stabilize the interferometer system. Besides, we propose an estimation algorithm to obtain the unavailable state and the signal of interest: the interferometer phase. These two approaches are put together to form the so-called *output feedback control*, in which we use the estimated signal for control. Our work's contribution relies on applying the nonlinear control and estimation theory for optical interferometry.

C. Outline

The remainder of this paper is as follows. Section II develops the Michelson interferometer dynamic model. The problem statement is given in Section III. This paper's main result is presented in three theorems given in Section IV. These theoretical results are afterward corroborated with numerical simulations in Section V. Finally, conclusions and final remarks are discussed in Section VI.

II. System description

A. Interferometer

One of the most outstanding interferometer configuration is *the Michelson interferometer* [19]. Michelson interferometer is used for detecting the length difference between two paths l_1 and l_2 by means of optical interference, see Fig. 1.

B. Michelson Interferometer model

The two-beam interferometric signal is modeled as [20]

$$I(t) = I_1(t) + I_2(t) + 2\sqrt{I_1(t)I_2(t)}\cos\left(\alpha_1(t) - \alpha_2(t)\right) \quad (1)$$

where t is the time, I_1 is the reference light intensity from the laser, I_2 is the intensity of the Doppler-shifted light returned from the sample surface, and $\alpha_1(t) - \alpha_2(t)$ is the interferometer phase. Equation (1) can be rewritten as [3]

$$I(t) = a_1(t) + a_2(t)\cos\left(\varphi(t)\right) \quad (2)$$

where the terms a_1 and a_2 represent the background and local contrast functions, respectively; and $\varphi(t) = \alpha_1(t) - \alpha_2(t)$ is the *searched* phase function. There is a trans-impedance circuit for changing the light signal into a voltage signal[2]. Then, a photodetector captures the interferometer's intensity. Thus, after this process, the signal (2) is represented as

$$v(t) = A + AV\cos\left(\varphi(t)\right). \quad (3)$$

In this voltage representation, A accounts for the laser power, photodiode responsivity, and amplifier gain, while V is the fringe visibility [12].

Now, let us consider the following assumptions [12].

Assumption 1: The terms A and V in (3) are constants.

Assumption 2: Terms (A, V) are considered known as they can be determined experimentally by a self-calibration procedure [21].

Assumption 1 permits to remove A from (3). Also, by Assumption 2 the equation (3) is rewritten as follows

$$v(t) = AV\cos\left(\varphi(t)\right) = -AV\sin\left(\varphi(t)\right). \quad (4)$$

Voltage (4) is filtered to compensate for fluctuations of the signal of interest $\varphi(t)$ under possible external disturbances, which usually occur at frequencies below 20 Hz. To this aim, a low pass filter can be used:

$$H(s) = \frac{Z_2(s)}{V(s)} = \frac{1}{1 + s/\omega_c}, \quad (5)$$

where ω_c is the cutoff frequency; s stands for Laplace transform complex variable; $V(s)$ is the input voltage ($v(t)$ in (4)) represented in the frequency domain; and $Z_2(s)$ is the output voltage in the frequency domain. Then, (5) can be represented in the time domain as follows

$$\frac{1}{\omega_c}\dot{z}_2(t) + z_2(t) = v(t). \quad (6)$$

with $v(t) = -AV\sin\left(\varphi(t)\right)$ from (4).

On the other hand, the phase displacement $\varphi(t)$ in (4) can be modeled as follows [19] pp. 115, [22] pp. 21:

$$\underbrace{\varphi(t)}_{z_1} = \frac{2\pi\chi}{\lambda}\Big(L\Delta n_s(t) + n_s(t)\Delta L(t)\Big) \quad (7)$$

where χ is the sensibility factor; λ is the wavelength of the laser light; $n_s(t)$ is the refractive index; L is the device length; $\Delta L(t) = l_2 - l_1$ is the variation of the interferometer length; and $\Delta n_s(t)$ represents the variation in the refractive index along the optical path traveled by the rays through the interferometer arms. Next, consider that the medium of propagation is the air, and then $n_s = 1$; also consider that there is no refractive index variation; moreover observe that

[2]The trans-impedance circuit allows the circuit-designer to turn light hitting a photodiode into an output voltage.

$\chi = 2$ for the Michelson interferometer since the laser beam passes two times along its arms, doubling the sensibility. Then (7) can be rewritten as $\varphi(t) = \frac{4\pi}{\lambda}\Delta L(t)$, where $\varphi(t) = z_1$ represents the total phase displacement at the interferometer input, being a function of the optical path difference between its two arms.

C. Interferometer model for control

To obtain the interferometer's dynamics, we consider the states (z_1, z_2) in (6) and (7). These states represent the phase displacement and the filtered output voltage measured by the photodetector, respectively. Thus (7) can be represented by

$$z_1 = \Delta\phi + \upsilon. \tag{8}$$

where υ is related to the control signal, and $\Delta\phi$ is the term of modulated phase containing the information about the displacement of the movable object of interest. The phase $\varphi(t)$ is modified by the *PZT actuator under evaluation* and by the *PZT feedback actuator* at reference arm, see Fig. 1 for the graphical description of the previous. The dynamics of (8) is given by

$$\dot{z}_1 = \underbrace{\dot{\Delta}\phi}_{\delta(t)} + \underbrace{\dot{\upsilon}}_{u}. \tag{9}$$

Then, from (4), (6), (7) and (9) the nonlinear system that models the interferometer is as follows

$$\begin{aligned} \dot{z}_1 &= u + \delta(t) \\ \dot{z}_2 &= -\underbrace{\frac{AV}{\tau}}_{a}\sin z_1 - \underbrace{\frac{1}{\tau}}_{b} z_2 \end{aligned} \tag{10}$$

where (z_1, z_2) are the system states; $1/\tau = \omega_c$, A and V are system parameters considered constants; and $\delta(t)$ is the time-derivative of the signal of interest. Also, observe that the unperturbed and open-loop system (system (10) when $\delta(t) = 0$ and $u = 0$) has an infinity number of equilibrium points.

III. Problem Statement

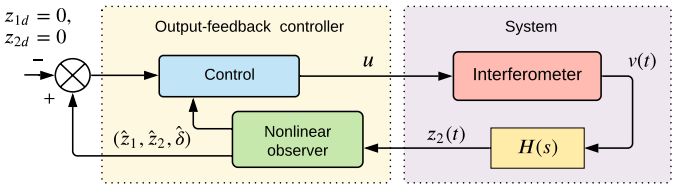

Fig. 2. Block diagram of the interferometer closed-loop system.

The interferometer's main purpose is to provide a way to measure the phase shift $\Delta\phi(t)$ at its input while providing stability to the system. Also, it is important to highlight that the state z_1 cannot be measured in real experiments, since the state $z_1 = \Delta\phi(t) + \upsilon$ contains the unknown and searched phase $\Delta\phi(t)$. However, a photodetector can measure z_2; see Fig. 1. Therefore, the problem can be summarized as follows.

Problem 1: Consider system (10) where it is only possible to measure the state z_2, i.e. it has output $y = z_2$. The challenges are:

- Stabilize the interferometer system (10) to any of the equilibrium points.
- Estimate $\delta(t)$ in (10) corresponding to the movable object.

Remark 1: The closed-loop system has infinite equilibrium points; this fact is desirable. As it is well known, it is extremely difficult to assemble a two beams interferometer (like a Michelson or Mach–Zehnder interferometer) with the reference and sensor arms of the same lengths. Therefore a static phase difference is always present. In other words, if the system is stable through an appropriate control technique, it will converge to any of those equilibrium points (usually to the nearest equilibrium for the unknown initial static length difference between the interferometer arms). Depending on the chosen actuator device (like PZT, fiber wound around cylindrical PZT, Pockels cell, IO phase shifter, among others), a considerable difficulty can occur in driving it from a starting point to a distant point from the origin (that is, the zero-order fringe). This is due to inherent problems related to the limited dynamic range for the actuators' optical phase variation.

IV. Main Results

This section presents our main results divided into three theorems: a) feedback control in which we assume that all states are available for feedback, b) a nonlinear observer to estimate the unknown states in the system (10), and c) using the two first results, an output feedback control to stabilize (10) to any of the stable equilibria.

A. Feedback control

Let consider the following assumption.

Assumption 3: The unknown phase shift has the first two time-derivatives bounded as follows

$$|\delta| \leq c, \quad \left|\dot{\delta}\right| \leq d \tag{11}$$

where $c, d \in \mathbb{R}^+$.

The first main result is summarized next.

Theorem 1: Consider system (10) and Assumption 3, also consider the controller given by[3]

$$u = -k\,\mathrm{sgn}\, z_1 - \kappa z_1 \tag{12}$$

where $k, \kappa \in \mathbb{R}^+$. Then the origin of the closed loop system (10)-(12) is globally exponentially stable (GES).

Proof: The proof is based on Lyapunov theory for variable structure systems [23]–[26]. Let a candidate Lyapunov function $V(z_1, z_2)$ be given by

$$V = \frac{1}{2}z_1^2 + \rho\,|z_2| \tag{13}$$

where $\rho \in \mathbb{R}^+$ is a free parameter. Thus one calculate the time derivative of the Lyapunov function $V(z_1, z_2)$ using (12) and

[3]Note that δ in (10) is considered unknown, and hence it does not appear in this control.

evaluate it in the trajectories of (10)

$$\begin{aligned}\dot{V} &= \frac{\partial V}{\partial z_1}\dot{z}_1 + \frac{\partial V}{\partial z_2}\dot{z}_2 \\ &= z_1\left(u+\delta\right) + \rho \operatorname{sgn} z_2\left(-a\sin z_1 - bz_2\right) \\ &= -k\left|z_1\right| - \kappa z_1^2 + \delta z_1 - \rho a \operatorname{sgn} z_2 \sin z_1 - \rho b\left|z_2\right| \\ &\leq -\left(k - c - \rho a\right)\left|z_1\right| - \rho b\left|z_2\right|\end{aligned} \tag{14}$$

since $|\delta| \leq c$ and inequalities $|\sin z_1| \leq |z_1|$, $|\operatorname{sgn} z_2| \leq 1$ hold. If $k > c + \rho a$ and $\rho > 0$, then $\dot{V} < 0\ \forall z \in \mathbb{R}^2 \setminus \{0\}$. Furthermore, $\dot{V} \leq -\eta V$ with $\eta = \min\{q, b\}$ on the arbitrarily large set $Q = \{z \in \mathbb{R}^2 \mid |z_1| \leq q\}$ where $q = 2(k - c - \rho a)$. Since the above differential inequality holds on the solution of the closed-loop system (10)-(12) on the set Q, V exponentially decays with decay rate η, i.e.

$$V(z_1(t), z_2(t)) \leq V(z_1(t_0), z_2(t_0)) \exp\left(-\eta(t - t_0)\right). \tag{15}$$

This proves that origin of the closed-loop system (10)-(12) is exponentially stable. As the Lyapunov function (13) is radially unbounded, i.e. $V(z) \to \infty$ as $\|z\| \to \infty$ then the closed-loop system is GES [27]. ■

B. Nonlinear observer

Recall that the variables $\delta(t)$ and z_1 cannot be measured, and hence control (12) cannot be implemented in practice. We propose a solution to this situation utilizing an observer.

Theorem 2: Consider system (10) where only the state z_2 is available, then the following system

$$\begin{aligned}\dot{\hat{z}}_1 &= -k \operatorname{sgn} \hat{z}_1 - \kappa \hat{z}_1 + \hat{\delta}(t) - \kappa_1\left(\hat{z}_2 - z_2\right) \\ \dot{\hat{z}}_2 &= -a\sin\left(\hat{z}_1\right) - b\hat{z}_2 - \kappa_2\left(\hat{z}_2 - z_2\right) \\ \dot{\hat{\delta}} &= -\kappa_3 \operatorname{sgn}\left(\hat{z}_2 - z_2\right) - \kappa_4\hat{\delta}\end{aligned} \tag{16}$$

is an observer for system (10) and hence the error solutions $e_1(t) = \hat{z}_1 - z_1$, $e_2(t) = \hat{z}_2 - z_2$ and $e_3(t) = \hat{\delta} - \delta$ are globally asymptotically stable.

Proof: The proof is based on Lyapunov stability analysis. Let us define the following errors between the original system states (10) and the estimate states (16): $e_1 = \hat{z}_1 - z_1$, $e_2 = \hat{z}_2 - z_2$ and $e_3 = \hat{\delta} - \delta$. The proof consists in obtaining the error dynamics from the last errors and determine that the errors converge to zero in some sense. Then, consider the following candidate C^1 Lyapunov function $\tilde{V} = V_1 + V_2 + V_3$ where $V_1 = l_1|e_1|$, $V_2 = l_2|e_2|$ and $V_3 = \frac{l_3}{2}e_3^2$ with $l_1, l_1, l_3 \in \mathbb{R}^+$. Now let us compute the time derivative of $\tilde{V}$ evaluated in the error trajectories defined above:

$$\begin{aligned}\dot{V}_1 &= \frac{\partial V_1}{\partial e_1}\frac{de_1}{dt} = l_1 \operatorname{sgn}(e_1)\left(\dot{\hat{z}}_1 - \dot{z}_1\right) \\ &= l_1 \operatorname{sgn}(e_1)\left(-k\left(\operatorname{sgn}\hat{z}_1 - \operatorname{sgn} z_1\right) - \kappa e_1 - \kappa_1 e_2 + e_3\right) \\ &\leq k l_1 \operatorname{sgn}(e_1)\left(\operatorname{sgn} z_1 - \operatorname{sgn}\hat{z}_1\right) - l_1\kappa|e_1| + \\ &\qquad l_1\kappa_1|e_2| + l_1|e_3| \\ &\leq -l_1\kappa|e_1| + l_1\kappa_1|e_2| + l_1|e_3|,\end{aligned} \tag{17}$$

the last inequality follows since $\operatorname{sgn}(\hat{z}_1 - z_1)\left(\operatorname{sgn} z_1 - \operatorname{sgn}\hat{z}_1\right) \leq 0$. We continue with $\dot{V}_2$ as follows.

$$\begin{aligned}\dot{V}_2 &= \frac{\partial V_2}{\partial e_2}\frac{de_2}{dt} = l_2 \operatorname{sgn}(e_2)\left(\dot{\hat{z}}_2 - \dot{z}_2\right) \\ &= l_2 \operatorname{sgn}(e_2)\left(a\sin z_1 - a\sin\hat{z}_1 - \varrho e_2\right) \\ &\leq l_2 a|e_1| - l_2\varrho|e_2|\end{aligned} \tag{18}$$

where $\varrho = b + \kappa_2$; also the last inequality follows from the Lipschitz property of the $\sin(\cdot)$ function. We proceed in the same manner for V_3

$$\begin{aligned}\dot{V}_3 &= \frac{\partial V_3}{\partial e_3}\frac{de_3}{dt} = l_3 e_3\left(\dot{\hat{\delta}} - \dot{\delta}\right) \\ &= l_3 e_3\left(-\kappa_3 \operatorname{sgn}(e_2) - \kappa_4(e_3 + \delta) - \dot{\delta}\right) \\ &\leq \left(\kappa_3 l_3 + \kappa_4 l_3 c + l_3 d\right)|e_3| - \kappa_4 l_3 e_3^2\end{aligned} \tag{19}$$

where we have used Assumption 3. Then, from (17), (18), and (19) it follows that

$$\begin{aligned}\dot{\tilde{V}} &\leq -l_1\kappa|e_1| + l_1\kappa_1|e_2| + l_1|e_3| + l_2 a|e_1| - l_2\varrho|e_2| + \\ &\qquad \left(\kappa_3 l_3 + \kappa_4 l_3 c + l_3 d\right)|e_3| - \kappa_4 l_3 e_3^2 \\ &\leq -\left(l_1\kappa - l_2 a\right)|e_1| - \left(l_2\varrho - l_1\kappa_1\right)|e_2| \\ &\qquad -\left(\kappa_4 l_3|e_3| - l_1 - \kappa_3 l_3 - \kappa_4 l_3 c - l_3 d\right)|e_3| \leq 0\end{aligned} \tag{20}$$

the last inequality holds as long as

$$|e_3| > \frac{l_1 + \kappa_3 l_3 + \kappa_4 l_3 c + l_3 d}{\kappa_4 l_3},\ l_1\kappa > l_2 a,\ l_2\varrho > l_1\kappa_1. \tag{21}$$

Notice that in the above part of the proof all the positive constants l_1, l_2, l_3, κ_1, κ_2, κ_3, κ_4, and κ are free parameters. Also, bounds (c, d) in (11) are given by the assumption 3. Then, the error states $(e_1(t), e_2(t), e_3(t))$ ultimately converge arbitrarily near to the origin, since it depends on the particular values of such constants; see (21).

To prove the asymptotic stability, we use the Lyapunov-Like Lemma, which results as a corollary from the Barbalat's Lemma [27]. The Lyapunov-Like Lemma basically claims that if: a) $\tilde{V}$ is lower bounded; b) $\dot{\tilde{V}}$ is at least negative semi-definite; and c) $\dot{\tilde{V}}$ is uniformly continuous in time, then $\dot{\tilde{V}} \to 0$ as $t \to \infty$. Let us verify such conditions for our Lyapunov function $\tilde{V}$ and its time derivative (20). First, let us consider the statement a). Observe that $\tilde{V}$ is lower bounded by the origin (this comes from the Lyapunov function definition). On the other hand, notice from (20) that $\dot{\tilde{V}}$ can be considered as negative semi-definite, thus condition b) is fulfilled. Finally, to prove c), let us consider the following lemma.

Lemma 1: If $\dot{f}(t)$ is bounded, then $f(t)$ is uniformly continuous.

Simple calculations yields that $\ddot{\tilde{V}}$ is bounded, since $\operatorname{sgn}(\cdot)$ is bounded and the states (e_1, e_2, e_3) were shown to be bounded. As a consequence, $\dot{\tilde{V}}$ is uniformly continuous and statement c) is proven. Hence, by the Lyapunov-Like Lemma $\dot{\tilde{V}} \to 0$ as $t \to \infty$, which in turn results that $(e_1, e_2, e_3) \to 0$ as $t \to \infty$. An asymptotic stability is proven. Finally, the global stability result comes from the fact that the Lyapunov function $\tilde{V}$ is radially unbounded. ■

Remark 2: For recovering $\Delta\phi(t)$ in (8), we need to calculate the time-integral of the obtained estimate $\hat{\delta}(t)$. This is due from the nature of (9).

C. Output feedback control analysis

As the reader can see, we have separately designed the control (12) and the observer (16) for system (10). This is possible thanks to the *separation principle*, which states that an observer and a control can be designed in a separate way, and then, be implemented together using the estimated states for feedback [28], [29]. We implement this approach called *output feedback control*.

Theorem 3: Suppose that assumptions 1, 2 and 3 hold and furthermore the control (12) makes the origin of system (10) globally exponentially stable. Then, the same system in closed-loop form with the feedback control

$$u = -k \operatorname{sgn} \hat{z}_1 - \kappa \hat{z}_1 \tag{22}$$

together with (16) achieves a practical stability.

Proof: Consider the following error dynamics together with the observer dynamics as follows:

$$\begin{aligned}
\dot{e}_1 &= -k\left(\operatorname{sgn}\hat{z}_1 - \operatorname{sgn} z_1\right) - \kappa e_1 - \kappa_1 e_2 + e_3 \\
\dot{e}_2 &= a \sin z_1 - a \sin \hat{z}_1 - \varrho e_2 \\
\dot{e}_3 &= -\kappa_3 \operatorname{sgn} e_2 - \kappa_4 \left(e_3 + \delta\right) - \dot{\delta} \\
\dot{\hat{z}}_1 &= \dot{z}_1 + \dot{e}_1 = -k \operatorname{sgn} \hat{z}_1 - \kappa \hat{z}_1 + \delta(t) - k \operatorname{sgn} \hat{z}_1 \\
&\qquad + k \operatorname{sgn} z_1 - \kappa e_1 - \kappa_1 e_2 + e_3 \\
\dot{\hat{z}}_2 &= \dot{z}_2 + \dot{e}_2 = -a \sin\left(\hat{z}_1 - e_1\right) - b\left(\hat{z}_2 - e_2\right) + a \sin z_1 \\
&\qquad - a \sin \hat{z}_1 - \varrho e_2.
\end{aligned} \tag{23}$$

Let us consider the following candidate Lyapunov function

$$W = K \underbrace{\left(\frac{1}{2}\hat{z}_1^2 + \rho\left|\hat{z}_2\right|\right)}_{V(\hat{z}_1,\hat{z}_2)} + \underbrace{l_1|e_1| + l_2|e_2| + \frac{l_3}{2}e_3^2}_{\tilde{V}(e_1,e_2,e_3)} \tag{24}$$

where $K > 0$; and $\tilde{V}$ is invoked from the observer's stability analysis.

Let us compute the time derivative of W in two parts. First, we start with the time derivative of $V(\hat{z}_1, \hat{z}_2)$ computed as follows:

$$\begin{aligned}
\dot{V} &= \hat{z}_1\dot{\hat{z}}_1 + \rho \operatorname{sgn}\left(\hat{z}_2\right)\dot{\hat{z}}_2 \\
&= \Big(-2k\left|\hat{z}_1\right| - \kappa\hat{z}_1^2 + \hat{z}_1\delta(t) + k\hat{z}_1 \operatorname{sgn} z_1 - \kappa\hat{z}_1 e_1 \\
&\quad - \kappa_1\hat{z}_1 e_2 + e_3\hat{z}_1\Big) + \rho\Big(-a \operatorname{sgn}\left(\hat{z}_2\right)\sin\left(\hat{z}_1 - e_1\right) \\
&\quad - b\left|\hat{z}_2\right| + be_2 \operatorname{sgn}\hat{z}_2 + a \sin z_1 \operatorname{sgn}\hat{z}_2 \\
&\quad - a \sin\hat{z}_1 \operatorname{sgn}\hat{z}_2 - \varrho e_2 \operatorname{sgn}\hat{z}_2\Big) \\
&\leq \Big(-k\left|\hat{z}_1\right| - \kappa\hat{z}_1^2 + c\left|\hat{z}_1\right| - \kappa e_1\hat{z}_1 - \kappa_1 e_2\hat{z}_1 + e_3\hat{z}_1\Big) \\
&\quad + \rho\Big(a\left|\hat{z}_1 - e_1\right| - b\left|\hat{z}_2\right| + b\left|e_2\right| + a\left|z_1 - \hat{z}_1\right| + \varrho\left|e_2\right|\Big) \\
&\leq -(k-c)\left|\hat{z}_1\right| - \kappa\hat{z}_1^2 - \rho b\left|\hat{z}_2\right| - \kappa e_1\hat{z}_1 - \kappa_1 e_2\hat{z}_1 \\
&\quad + e_3\hat{z}_1 + \rho a\left|\hat{z}_1 - e_1\right| + \rho a\left|e_1\right| + \rho(b+\varrho)\left|e_2\right|.
\end{aligned} \tag{25}$$

Then, the time-derivative of $\tilde{V}$ in (24) is based on $\dot{\tilde{V}}(e_1, e_2, e_3)$ already computed in (20). Consequently, the time-derivative of W of (24) uses (20) and (25) and results in

$$\begin{aligned}
\dot{W} &= K\dot{V}(\hat{z}_1, \hat{z}_2) + \dot{\tilde{V}}(e_1, e_2, e_3) \\
&\leq -K(k-c)\left|\hat{z}_1\right| - K\kappa\hat{z}_1^2 - K\rho b\left|\hat{z}_2\right| \\
&\quad - K\kappa e_1\hat{z}_1 - K\kappa_1 e_2\hat{z}_1 + Ke_3\hat{z}_1 \\
&\quad + K\rho a\left|\hat{z}_1 - e_1\right| + K\rho a\left|e_1\right| + K\rho(b+\varrho)\left|e_2\right| \\
&\quad - (l_1\kappa - l_2 a)\left|e_1\right| - (l_2\varrho - l_1\kappa_1)\left|e_2\right| \\
&\quad - \Big(\kappa_4 l_3|e_3| - l_1 - \kappa_3 l_3 - \kappa_4 l_3 c - l_3 d\Big)|e_3|.
\end{aligned} \tag{26}$$

Once we arranged all the terms in (26) it follows that

$$\begin{aligned}
\dot{W} &\leq -K\left(k - c - \rho a - \kappa\left|e_1\right| - \kappa_1\left|e_2\right| - \kappa_1\left|e_3\right|\right)\left|\hat{z}_1\right| \\
&\quad - K\kappa\hat{z}_1^2 - K\rho b\left|\hat{z}_2\right| - \Big(l_1\kappa - l_2 a - 2K\rho a\Big)|e_1| \\
&\quad - \Big(l_2\varrho - l_1\kappa_1 - K\rho(b+\varrho)\Big)|e_2| \\
&\quad - \Big(\kappa_4 l_3|e_3| - l_1 - \kappa_3 l_3 - \kappa_4 l_3 c - l_3 d\Big)|e_3|.
\end{aligned} \tag{27}$$

Therefore the closed-loop system achieves practical stability as long as we choose sufficiently large gains such that $k > c + \rho a + \kappa \sup|e_1| + \kappa_1 \sup|e_2| + \kappa_1 \sup|e_3|$, $l_1\kappa > l_2 a + 2K\rho a$, $l_2 > \frac{l_1\kappa_1}{\varrho} + \frac{K\rho b}{\varrho} + K\rho$, and (21) hold. ■

V. Simulations

In this Section we conduct several simulation using MATLAB and demonstrate that the results corroborate the above theory. For the simulation, we use the following system parameters: $a = 7$, $b = 3$, and $\delta = \sin\left(0.6\cos\left(t - e^{0.34t}\right)\right) + 0.5\cos\left(0.8t + e^{0.1t}\right) + 0.6\arctan\left(t\right) - 1.8\exp\left(-2t\right) - 0.26$. The control parameters are $k = 18$, $\kappa = 5$, $\kappa_1 = 20000$, $\kappa_2 = 10000$, $\kappa_3 = 7.8$, and $\kappa_4 = 4.6$.

Let us consider Fig. 3, where trajectories of system (10) together with the output feedback control (16)-(22) are shown. Note that z_1 converges to any of the stable equilibrium points, while $z_2 \to 0$. States behavior present notable robust capabilities since the states converge despite an unknown signal $\delta(t)$. Observe that z_1 converges to different equilibria depending on its initial conditions, as expected and desired; see Remark 1.

The results of the observer are depicted in Fig. 4. The observer's goal is to estimate the original states (z_1, z_2) and the augmented state $\hat{\delta}$. The latter represents an estimate of the unknown signal $\delta(t)$. The signal $\delta(t)$ is correctly estimated without any large output during transients.

VI. Conclusion

In this paper, a nonlinear control that stabilizes an interferometer system was presented. Moreover, a nonlinear observer was designed to estimate the interferometer states and the unknown signal $\delta(t)$. This paper's work did not account for the nonlinearity inherent to the piezoelectric actuator, such as hysteresis [30], and creep [31]. This is due to the application conditions, i.e., the interferometry application was in a high-frequency sinusoidal signal with which these behaviors are

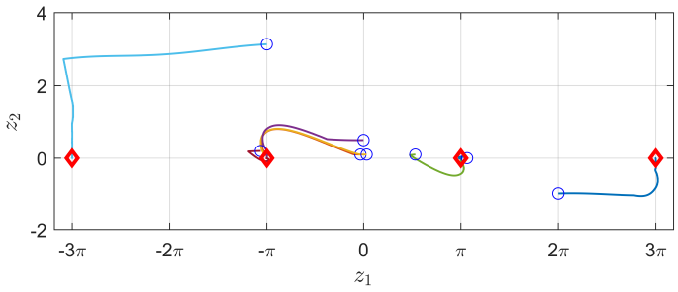

Fig. 3. Phase portrait of the proposed closed-loop system with the output feedback control. Red diamonds are equilibrium points; empty circles are the initial conditions.

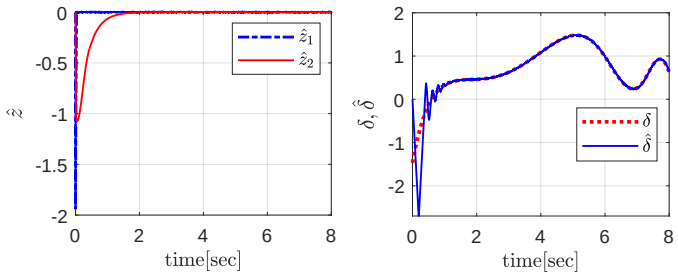

Fig. 4. At the left, estimated states behavior $\hat{z} = [\hat{z}_1, \hat{z}_2]^\intercal$ with initial conditions at the origin. At the right, observer convergence to signal of interest $\delta(t)$; observe how after a transient time, $\hat{\delta}(t)$ converges to the real value $\delta(t)$.

lessened. Future works will introduce these PZT actuator nonlinearities in order to provide better precision performance.

Up to our knowledge, such a work is one of the first that introduces state feedback nonlinear control to the interferometry, which opens an opportunity to research between two areas of science: optics and advanced control theory.

REFERENCES

[1] R. Oudmaijer, C. Haniff, D. Buscher, and J. Young, "Optical interferometry - the sharpest tool in the box," *Astronomy & Geophysics*, vol. 53, no. 2, pp. 2.14–2.18, 2012.

[2] The Event Horizon Telescope Collaboration, "First M87 Event Horizon Telescope Results. II. Array and Instrumentation," *The Astrophysical Journal Letters*, vol. 875, no. 1, p. L2, Apr. 2019.

[3] M. Servin, J. Quiroga, and J. Padilla, *Fringe pattern analysis for optical metrology*. Germany: Wiley-VCH, 2014.

[4] K. Fritsch and G. Adamovsky, "Simple circuit for feedback stabilization of a single-mode optical fiber interferometer," *Review of Scientific Instruments*, vol. 52, no. 7, pp. 996–1000, Jul. 1981.

[5] R. G. White and D. C. Emmony, "Active feedback stabilisation of a Michelson interferometer using a flexure element," *Journal of Physics E: Scientific Instruments*, vol. 18, no. 8, pp. 658–663, aug 1985.

[6] D. C. L. Cheung, T. H. Barnes, and T. G. Haskell, "Feedback interferometry with membrane mirror for adaptive optics," *Optics Communications*, vol. 218, no. 1, pp. 33–41, Mar. 2003.

[7] A. D. Fisher and C. Warde, "Simple closed-loop system for real-time optical phase measurement," *Optics Letters*, vol. 4, no. 5, pp. 131–133, May 1979, publisher: Optical Society of America.

[8] D. Nakane, T. A. Wheatley, D. W. Berry, H. Yonezawa, H. Arao, D. T. Pope, T. C. Ralph, H. M. Wiseman, E. H. Huntington, and A. Furusawa, "Adaptive optical phase estimation," in *CLEO/QELS: 2010 Laser Science to Photonic Applications*, May 2010, pp. 1–2.

[9] G. Jotzu, T. J. Bartley, H. B. Coldenstrodt-Ronge, B. J. Smith, and I. A. Walmsley, "Continuous phase stabilization and active interferometer control using two modes," *Journal of Modern Optics*, vol. 59, no. 1, pp. 42–45, Jan. 2012.

[10] M. Böhm, M. Glück, A. Keck, J.-U. Pott, and O. Sawodny, "Improving the performance of interferometric imaging through the use of disturbance feedforward," *Journal of the Optical Society of America A*, vol. 34, no. 5, p. A10, May 2017.

[11] A. Patil, B. Raphael, and P. Rastogi, "Introduction of stochastic methods to phase-shifting interferometry," *Journal of Modern Optics*, vol. 52, no. 1, pp. 33–44, Jan. 2005.

[12] R. I. Martin, J. M. S. Sakamoto, M. C. M. Teixeira, G. A. Martinez, F. C. Pereira, and C. Kitano, "Nonlinear control system for optical interferometry based on variable structure control and sliding modes," *Optics Express*, vol. 25, no. 6, pp. 6335–48, 2017.

[13] D.-U. Kam, J. H. Kim, and K. Lee, "Unwrapped phase correction for robust 3d scanning," *Applied Optics*, vol. 58, no. 14, pp. 3676–3684, May 2019.

[14] I. Choque, M. Servin, M. Padilla, M. Asmad, and S. Ordones, "Phase measurement of nonuniform phase-shifted interferograms using the frequency transfer function," *Applied Optics*, vol. 58, no. 15, pp. 4157–4162, May 2019.

[15] P. Hariharan, *Optical interferometry*, 2nd ed. Amsterdam: Acad. Press, 2003.

[16] ——, *Basics of interferometry*, 2nd ed. Amsterdam: Elsevier Academic Press, 2007.

[17] Y. Shtessel, C. Edwards, L. Fridman, and A. Levant, *Sliding Mode Control and Observation*. Birkhäuser Basel, 2014.

[18] S. Alvarez-Rodríguez, G. Flores, and N. A. Ochoa, "Variable Gains Sliding Mode Control," *International Journal of Control, Automation and Systems*, vol. 17, no. 3, pp. 555–564, Mar. 2019.

[19] E. Udd and W. B. S. Jr., *Fiber Optic Sensors: An Introduction for Engineers and Scientists*. Wiley, 2011.

[20] X. H. Chen, X. L. Zeng, D. Fan, Q. C. Liu, B. X. Bie, X. M. Zhou, and S. N. Luo, "Note: Phase retrieval method for analyzing single-phase displacement interferometry data," *Review of scientific instruments*, vol. 85, no. 026106, pp. 1–3, 2014.

[21] J. Xu, Q. Xu, L. Chai, Y. Li, and H. Wang, "Direct phase extraction from interferograms with random phase shifts," *Optics Express*, vol. 18, no. 20, pp. 20 620–20 627, 2010.

[22] R. I. Martin, "Nonlinear control system based on variable structure and sliding modes for two beam optical interferometry," Ph.D. dissertation, Unesp - Universidade Estadual Paulista, Ilha Solteira, Brazil, 2018.

[23] J. Cortés, "Discontinuous dynamical systems. a tutorial on solutions, nonsmooth analysis and stability," *IEEE Control Systems Magazine*, vol. 28, no. 3, pp. 36–73, 2008.

[24] V. I. Zubov, *Methods of A. M . Lyapunov and their application*. P. Noordhoff, 1964.

[25] S. Sastry, *Nonlinear Systems: Analysis, Stability, and Control*. USA: Springer, 1999.

[26] H. K. Khalil, *Nonlinear Systems*. USA: Prentice Hall, 2002.

[27] J.-J. E. Slotine and W. Li, *Applied nonlinear control*. Prentice Hall, 1991.

[28] A. N. Atassi and H. K. Khalil, "A separation principle for the stabilization of a class of nonlinear systems," *IEEE Transactions on Automatic Control*, vol. 44, no. 9, pp. 1672–1687, Sep. 1999.

[29] A. Atassi and H. Khalil, "A separation principle for the control of a class of nonlinear systems," *IEEE Transactions on Automatic Control*, vol. 46, no. 5, pp. 742–746, May 2001.

[30] M. Rakotondrabe, "Multivariable classical Prandtl-Ishlinskii hysteresis modeling and compensation and sensorless control of a nonlinear 2-dof piezoactuator," *Nonlinear Dynamics*, 2017.

[31] ——, "Modeling and compensation of multivariable creep in multi-dof piezoelectric actuators," *IEEE International Conference on Robotics and Automation*, pp. 4577–4581, 2012.